# Identifiability from a single dispersion branch in a two-field effective theory

**Abstract**

We study an inverse problem for a stable two-field quadratic system with derivative mixing and an independent spatial stiffness. The system has a Lorentz-invariant scalar realization in which a determinant operator vanishes on every homogeneous configuration. We distinguish a fixed-background-action comparison from inference with unknown spectral parameters. In the latter problem, three measurements of the light pole at distinct positive squared momentum magnitudes uniquely determine the three spectral parameters away from one exceptional locus; two measurements are locally insufficient. On that locus the entire light branch is exactly linear despite nonzero mixing, and a continuous family of heavy scales remains indistinguishable from light-pole positions alone. One heavy-gap measurement or one calibrated source-residue measurement resolves the ambiguity. Equivalent low-momentum reconstruction formulas expose the singular conditioning near the exceptional locus. We give explicit error propagation and finite-fit truncation bounds. The statements concern the specified classical action and declared observation model; they do not bound unknown higher operators or imply a UV completion.

## 1 Introduction

Homogeneous evolution generally does not fix the dynamics of perturbations. In effective field theories this distinction is explicit in the separation between background terms and higher-order fluctuation operators [1]. For several scalar fields, antisymmetrized kinetic invariants provide a particularly direct example: they vanish when all gradients are parallel, while contributing to spatial perturbations [2, 3]. Neither this mechanism nor the forward dispersion of a derivative-mixed two-field system is new [4–7]. The present question is an inverse one: how much information about the two-field system is contained in only its light dispersion branch?

We give a complete answer within a three-parameter classical spectral model. The central result classifies all light-branch data fibres and proves a minimal finite-data statement. It also separates structural identifiability from stable recovery: an inverse may exist while small errors prevent a useful determination of the heavy scale. The exceptional case is not a decoupling limit. Its mixing is nonzero, its complete light dispersion is exactly linear, and its calibrated response residues still contain the missing information. Figure 1 displays the distinction between pole locations and calibrated response weights.

The general quadratic action in Ref. [6, eqs. (61)–(63)] already allows independent propagation coefficients and single-derivative mixing. More directly, Ref. [7, eqs. (4.17), (4.21)] gives the full flat-space propagator and unequal-speed poles. Its spectral polynomial becomes ours under the algebraic substitutions $k^2_{\mathrm{ref}} = ax$, $c^2_{s,\mathrm{ref}} = 1/a$, $m^2_{\mathrm{ref}} = M$ and $\rho^2_{\mathrm{ref}} = N$. This compares formulas; it does not change the reference metric of the present model. We claim no new forward action or propagator.

Our result is the inverse-data classification, including its complete interior exception and a response datum that resolves it. It differs from degeneracies of cosmological observables under approximations [8] and from nonunique covariant completions of given background and

linear dynamics [9]. We neither solve those larger reconstruction problems nor propose a new general system-identification method.

## 2 Model, observations and two different inverse problems

In four spacetime dimensions use signature $(+---)$ and a fixed reference metric $\eta_{\mu\nu}$. Define

$$Y_s = (\partial\sigma)^2, \qquad Y_t = (\partial\theta)^2, \qquad Z = \partial\sigma \cdot \partial\theta. \tag{1}$$

The scalar action is

$$\mathcal{L}_C = \frac{1}{2}Y_s + \frac{1}{2}(1+g\sigma)Y_t - \frac{1}{2}gv^2\sigma - \frac{1}{2}m^2\sigma^2 + C(Z^2 - Y_sY_t). \tag{2}$$

It has a constant $\theta$ shift, a $\theta$ reflection, spacetime parity and Poincare symmetry. We work locally in $1+g\sigma > 0$, with $m^2 > 0$ and $gv \neq 0$. The two scalar fields have mass dimension one; $[v] = 2$, $[g] = -1$, $[C] = -4$. For stress comparisons, all members use the same minimal continuation to an external source metric, without parameter-dependent curvature improvements.

The configuration $\sigma_0 = 0$, $\theta_0 = vt$ is an exact scalar solution. The kinetic force in the $\sigma$ equation cancels the specified potential gradient. Its energy density and pressure are $\rho = p = v^2/2$. Gravity is nondynamical; this is not an Einstein–Minkowski solution with only the stated matter.

For $\sigma = s$ and $\theta = vt + \pi$, set

$$D = gv, \quad M = m^2, \quad N = D^2, \quad B = M + N, \quad r = \frac{M}{B}, \quad q = 1 - r, \quad a = 1 - 2Cv^2. \tag{3}$$

The admissible spectral domain is

$$\mathcal{P} = \{(a, B, r) : a > 0,\ B > 0,\ 0 < r < 1\}. \tag{4}$$

Up to a linear boundary term, the full quadratic Lagrangian is

$$\mathcal{L}_2 = \frac{1}{2}(\dot{s}^2 + \dot{\pi}^2) - \frac{1}{2}[a(\nabla s)^2 + (\nabla\pi)^2] - \frac{1}{2}Ms^2 + Ds\dot{\pi}. \tag{5}$$

The derivative mixing is retained. The potential cross term vanishes by the shift symmetry. The canonical Hamiltonian,

$$\mathcal{H}_2 = \frac{1}{2}p_s^2 + \frac{1}{2}(p_\pi - Ds)^2 + \frac{1}{2}a(\nabla s)^2 + \frac{1}{2}(\nabla\pi)^2 + \frac{1}{2}Ms^2, \tag{6}$$

is positive definite at nonzero momentum. The zero-momentum shift mode is not an asymptotic-stability claim.

**Problem I: a known homogeneous action.** Fix $m, g, v$ and vary only $C$. All homogeneous actions and their scalar and metric first variations coincide, since $Z^2 - Y_sY_t$ and its first variations vanish on collinear gradients. Thus $B, r$ are fixed in this comparison. A single additional suitable spatial-response datum determines $a$.

**Problem II: unknown spectral parameters.** Keep the action form and the calibrated reference metric, $v$ and field/source normalization fixed, but infer the unknown triple $(a, B, r)$ from light-pole positions. Changing $B$ at fixed $r$ changes $m$ and $|g|$, hence the full homogeneous action. Such models may share the chosen rolling solution and its $\rho, p$, but they do not share every homogeneous off-shell history. Theorems below refer to Problem II unless stated otherwise. The signs of $D$ and $g$ are not determined by pole positions.

## 3 Forward spectrum and useful inequalities

Let $x = k^2 \geq 0$, $y = \omega^2$. The inverse kernel and its determinant are

$$P(\omega, k) = \begin{pmatrix} y - ax - M & -iD\omega \\ iD\omega & y - x \end{pmatrix}, \tag{7}$$

$$F(y, x) = y^2 - [B + (a+1)x]y + ax^2 + rBx. \tag{8}$$

The two poles are

$$y_\pm(x) = \frac{B + (a+1)x \pm \sqrt{\Delta(x)}}{2}, \quad \Delta(x) = B^2 + 2B(a + 1 - 2r)x + (a-1)^2x^2. \tag{9}$$

To see positivity directly, put $u = ax + M > 0$. Then $\Delta = (u - x)^2 + 2N(u + x) + N^2 > 0$. The pole sum is positive and their product is $ax^2 + Mx > 0$ for $x > 0$, so both poles are positive; at $x = 0$ they equal $0, B$. Moreover

$$F(x, x) = -Nx < 0 \quad \Longrightarrow \quad 0 < y_-(x) < x < y_+(x). \tag{10}$$

Consequently the measured light phase-velocity square $z(x) = y_-(x)/x$ satisfies $0 < z < 1$ and obeys

$$x(1 - z)(a - z) = B(z - r), \qquad z'(x) = \frac{(1 - z)(a - z)}{B + x(a + 1 - 2z)}. \tag{11}$$

The denominator equals $\sqrt{\Delta} > 0$. Continuity from $z(0) = r$ and Eq. (11) exclude crossing $a$ or 1 when $a \neq r$. If $a > r$, $z$ lies between $r$ and $\min(a, 1)$ and is strictly increasing. If $a < r$, it lies between $a$ and $r$ and is strictly decreasing. If $a = r$, it is constant.

## 4 Minimal light-pole data and the exceptional fibre

**Theorem 1** (Finite-data identifiability)**.** *Within $\mathcal{P}$, three lower-pole measurements $y_i = y_-(x_i)$ at any three distinct $x_i > 0$ uniquely determine $(a, B, r)$ whenever $a \neq r$. Two such scalar measurements are locally insufficient at every interior point off this locus. On $a = r$, the complete light branch is $y_-(x) = rx$, independently of $B > 0$. Its full data fibre is exactly $\{(r, B, r) : B > 0\}$ for fixed measured slope $r$.*

*Proof.* Put $z_i = y_i/x_i$. Equation (8) is linear in $(a, B, M)$:

$$A \begin{pmatrix} a \\ B \\ M \end{pmatrix} = f, \quad A_{i\cdot} = [x_i(1 - z_i), -z_i, 1], \quad f_i = x_i z_i (1 - z_i). \tag{12}$$

For model data, the first entry of each row is

$$x_i(1 - z_i) = -B + \frac{B(a - r)}{a - z_i}. \tag{13}$$

When $a \neq r$, monotonicity makes all $z_i$ distinct and none equals $a$. Adding $B$ times column three to column one reduces the determinant to $B(a - r)$ times that of the columns $[1/(a - z_i), -z_i, 1]$. Multiplying row $i$ by $a - z_i$ gives columns $[1, z_i^2 - az_i, a - z_i]$, an invertible polynomial change of the Vandermonde columns $[1, z_i, z_i^2]$. In particular,

$$\det A = B(a - r)\frac{\prod_{i<j}(z_j - z_i)}{\prod_i (a - z_i)}. \tag{14}$$

Thus $A$ is nonsingular. Every admissible model fitting the same three data must solve this same linear system, proving global uniqueness.

With only two nodes the rows have rank two: they could be proportional only if, because their final entries equal one, the $z_i$ were equal. The solution set is therefore an affine line in $(a, B, M)$. In a sufficiently small neighborhood of an interior true point, the strict inequalities $a > 0$ and $B > M > 0$ persist. The fixed measured roots still satisfy $0 < y_i < x_i$; since $F(x_i, x_i) = -(B - M)x_i < 0$ for the alternative admissible parameters, they remain the lower roots. A continuum of admissible models fits the two observations.

At $a = r$, direct factorization gives

$$F(y, x) = (y - rx)(y - B - x), \tag{15}$$

so the lower root is $rx$ for all $x \geq 0$. Conversely, observations $y_i = rx_i$ at two distinct positive nodes impose $a = r$ and $M = rB$ through (8); $B$ remains free. This also proves completeness of the stated exceptional fibre. □

The parameter count is a count of scalar pole-location measurements at fixed, known momenta. It does not exclude a single composite observable that itself encodes multiple independent data, nor does it certify that an arbitrary measured dispersion belongs to this model. Additional observations provide model-consistency tests.

### 4.1 Equivalent local and partially calibrated data

The expansion of the light branch is

$$y_-(x) = rx + bx^2 + cx^3 + O(x^4), \qquad b = \frac{q(a - r)}{B}, \qquad c = \frac{b(2r - a - 1)}{B}. \tag{16}$$

For $b \neq 0$, write $d = b^2 + qc$. Then

$$B = -\frac{bq^2}{d}, \qquad a = r + \frac{Bb}{q}, \qquad M = rB, \quad N = qB. \tag{17}$$

Indeed $d = -bq^2/B$. Thus the light $k^6$ jet is generically sufficient, whereas $(r, b)$ leaves the continuum $a = r + Bb/q$ on its admissible interval. The exception is $b = 0$, not $c = 0$: for $r > 1/2$, $a = 2r - 1$ has $c = 0$ but $b \neq 0$ and is reconstructible.

If $r$ is independently known, two finite light-pole observations suffice off $a = r$. Define

$$h_i = \frac{z_i - r}{x_i(1 - z_i)}. \tag{18}$$

Then

$$B = \frac{z_2 - z_1}{h_1 - h_2}, \qquad a = z_1 + Bh_1. \tag{19}$$

If both $B, r$ are known, as in Problem I, one finite pole determines

$$a = \frac{y^2 - (B + x)y + rBx}{x(y - x)}. \tag{20}$$

The denominator is nonzero by (10). There is no unidentified heavy-scale fibre in that one-parameter experiment.

## 5 Resolving the exceptional fibre with a calibrated response

Measuring the heavy gap immediately determines $B$. A different option is a response measurement with a calibrated linear probe, defined by adding $-J_\theta\pi$ to the fluctuation Lagrangian. The linear equation is then $P(s,\pi)^T = (0, J_\theta)^T$, so $G_{\theta\theta} = \delta\pi/\delta J_\theta$ is the $\theta\theta$ component of $P^{-1}$ with the retarded frequency prescription. The probe and its normalization transform together with the field under any change of variables. At zero source the action is unchanged. Algebraically,

$$G_{\theta\theta}(y,x) = \frac{y - ax - M}{F(y,x)}. \tag{21}$$

On $a = r$, its light-pole residue with respect to $y$ is

$$R_\theta(x) = \frac{rB}{B+qx}, \qquad B = \frac{qxR_\theta}{r - R_\theta}, \quad x > 0. \tag{22}$$

A residue with respect to positive frequency $\omega$ equals $R_\theta/(2\omega_-)$ and must be converted accordingly. The result concerns this calibrated source response; an unknown multiplicative response normalization can absorb the change of $B$ in a single residue measurement at one momentum and invalidate that inversion. A whole response curve with one shared unknown normalization is a different data problem.

Even with perfect calibration, the relative sensitivity is

$$\left|\frac{R_\theta}{B}\frac{\partial B}{\partial R_\theta}\right| = \frac{r}{r - R_\theta} = 1 + \frac{B}{qx}. \tag{23}$$

Thus exact identifiability is not uniform robustness at low momentum or weak mixing. In an EFT reading with $|Cv^2| \ll 1$, the exceptional relation requires $q = 2Cv^2 \ll 1$, which can make the required residue precision particularly demanding. In a usable window $x \le X_{\max}$, the sensitivity is at least $1 + B/(qX_{\max})$; a well-conditioned window below the EFT cutoff is therefore not guaranteed.

## 6 Conditioning and controlled finite fits

At fixed $r$, the inverse (17) satisfies

$$\frac{\partial B}{\partial c} = \frac{B^2}{bq}, \qquad \frac{\partial B}{\partial b} = \frac{B}{b} + \frac{2B^2}{q^2}. \tag{24}$$

Absolute coefficient errors are amplified as $b \to 0$ at finite $B, r$. With $r, b$ held fixed in the derivative and $B$ held at its baseline value only in the normalization, the dimensionless local sensitivity is $|\partial B/\partial c|/B^3 = 1/[q^2|a - r|]$. Figure 2 illustrates this divergence. Appendix D gives a directly computable finite-data matrix certificate, without a Taylor fit. To state a finite bound, suppose $|\delta r| \le \epsilon_r$, $|\delta b| \le \epsilon_b$, $|\delta c| \le \epsilon_c$. Define

$$E_d = 2|b|\epsilon_b + \epsilon_b^2 + q\epsilon_c + |c|\epsilon_r + \epsilon_r\epsilon_c, \tag{25}$$

$$\eta = E_d/|d|, \qquad U = (1 + \epsilon_b/|b|)(1 + \epsilon_r/q)^2 - 1. \tag{26}$$

If $b \neq 0$, $\epsilon_r < q$ and $\eta < 1$, then

$$\left|\frac{\widehat{B}}{B} - 1\right| \le \frac{U + \eta}{1 - \eta}. \tag{27}$$

This follows by bounding the numerator factors in $\widehat{B}/B = (\widehat{b}/b)(\widehat{q}/q)^2(d/\widehat{d})$. The recovered domain conditions $0 < \widehat{r} < 1$, $\widehat{B} > 0$ and $\widehat{a} > 0$ must also be checked.

A pointwise Taylor remainder alone does not bound fitted coefficients. Appendix B supplies an explicit three-node fitting design and its inverse norm. For $x_i = ih$, an absolute error $\epsilon_y$ in each pole value and a verified bound $|y_-^{(4)}| \le K_4$ on $[0, 3h]$ imply

$$\epsilon_r \le \frac{29\epsilon_y}{6h} + \frac{9}{4}K_4 h^3, \tag{28}$$

$$\epsilon_b \le \frac{5\epsilon_y}{h^2} + \frac{25}{8}K_4 h^2, \tag{29}$$

$$\epsilon_c \le \frac{7\epsilon_y}{6h^3} + \frac{11}{12}K_4 h. \tag{30}$$

The tradeoff between truncation and measurement error is explicit. A rigorous $K_4$ requires independently justified parameter bounds; it cannot be certified by an unvalidated fit alone.

## 7 Interpretation and limits

Theorem 1 is an exact inverse statement for the classical action (2) and its stated observations. It uses known forward physics. The equality of complete homogeneous sectors applies only to Problem I; the exceptional inverse fibre of Problem II is a different statement about partial spectral data.

Regular field-coordinate changes preserve principal characteristics by congruence. Equivalence requires consistent transformation of induced operators and sources [10]. Stationary linearized derivative changes with an invertible symbol preserve physical finite poles when all induced terms and source transformations are retained. Corresponding background states and the physical time/shift generator must also be identified. An unaccompanied field rescaling does not preserve a calibrated response amplitude, and arbitrary maps between unrelated backgrounds are outside the comparison. The boundary cases $M = 0$, $N = 0$ or $a = 0$ are excluded from the open parameter domain; no completeness statement about their additional degeneracies is intended.

For a local EFT interpretation, require $m, |D|, |k|, |\omega| \ll \Lambda$, $|v|/\Lambda^2 \ll 1$, $|Cv^2| \ll 1$, and small perturbations in the local field domain. No quantitative bound on omitted Wilson coefficients or loops follows from these statements alone. The data-error bounds above can include a separately justified model-discrepancy bound; they do not manufacture one. A finite cutoff also prevents interpreting formal $k \to \infty$ characteristics as a proved UV front speed. The tuned surface $a = r$ is not asserted to be radiatively protected or generic. No cosmological, photon, gravitational-wave or observational identification is made.

## 8 Conclusion

The complete light dispersion is generically sufficient to identify the three spectral parameters of this two-field model, and three light-pole measurements at distinct positive squared momentum magnitudes are minimal. The unique admissible exception is an exactly linear light branch with nonzero mixing and an arbitrary heavy scale. A calibrated response residue or a gap measurement supplies the missing information. The explicit inverse formulas show why the generic limit near this exception is ill conditioned, and the finite-fit bounds state what precision assumptions are needed for a quantitative reconstruction.

## A Homogeneous restriction and the local scalar realization

For collinear gradients $\partial_\mu\sigma = un_\mu$, $\partial_\mu\theta = wn_\mu$, put $H = g^{\mu\nu}n_\mu n_\nu$. Then $Y_s = u^2H$, $Y_t = w^2H$, $Z = uwH$, so $O = Z^2 - Y_sY_t = 0$. Its field-gradient and metric first derivatives vanish

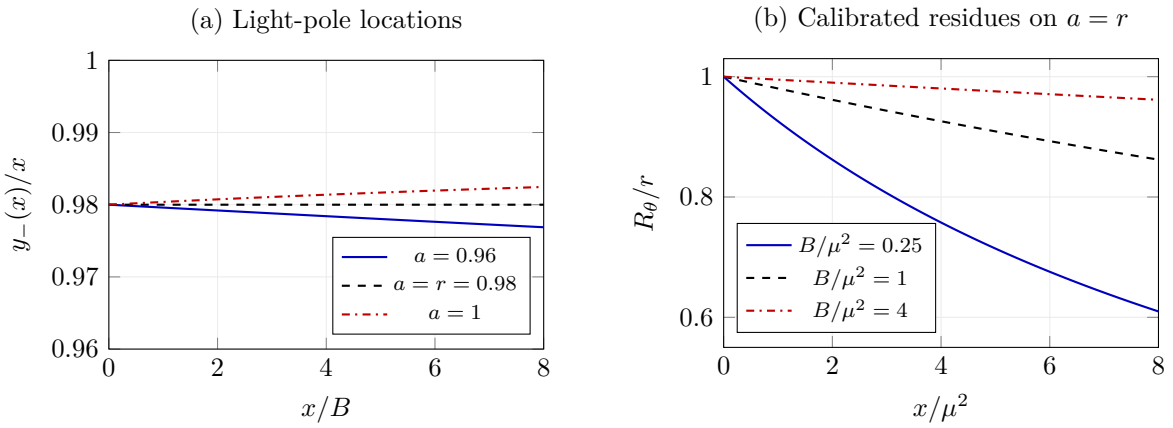



Figure 1: Exact classical model curves with $r = 0.98$. (a) At fixed $B$, the light phase-velocity square varies monotonically for $a \neq r$ and is constant at $a = r$. The value at $x = 0$ denotes its continuous limit. (b) On the exceptional locus, all heavy scales have the same light-pole curve $y_- = rx$, while the normalized calibrated residues distinguish $B$. Here $\mu$ is a common arbitrary reference mass, not a fitted heavy scale. These are model illustrations, not empirical data or error bounds for omitted EFT operators.

separately. Thus Problem I preserves the full homogeneous scalar equations and the stress defined by the common minimal metric-source prescription.

In the parity-even four-first-derivative basis $\{Y_s^2, Y_t^2, Y_sY_t, Z^2\}$, homogeneous restriction has rank three over constant coefficients and kernel generated by $(0, 0, -1, 1)$. Allowing coefficient functions of $\sigma$ gives a rank-one module. This is not a classification of all operators involving Hessians or curvature, nor a claim that the displayed truncation is closed under field redefinitions or renormalization.

## B Pointwise remainder and finite-fit amplification

Write $\zeta = a + 1 - 2r$. Differentiating the exact lower pole yields

$$y_-'' = \frac{2B^2q(a-r)}{\Delta^{3/2}}, \tag{31}$$

$$y_-''' = -\frac{3B^2q(a-r)\Delta'}{\Delta^{5/2}}, \tag{32}$$

$$y_-'''' = \frac{3B^2q(a-r)[\frac{5}{2}(\Delta')^2 - \Delta''\Delta]}{\Delta^{7/2}}. \tag{33}$$

On $0 \le x \le X$, suppose $\Delta \ge \Delta_{\min} > 0$, $|\Delta'| \le L_1$, and $\Delta \le \Delta_{\max}$. Then one valid bound is

$$K_4 = \frac{3B^2q|a-r|[\frac{5}{2}L_1^2 + 2(a-1)^2\Delta_{\max}]}{\Delta_{\min}^{7/2}}. \tag{34}$$

Taylor's theorem gives $|y_- - rx - bx^2 - cx^3| \le K_4x^4/24$. These constants can be bounded conservatively on a specified compact parameter set; no prior-independent uncertainty guarantee is asserted.

For $x_i = ih$, let $z_i = y_i/x_i$. Quadratic interpolation of $z$ gives

$$\widehat{r} = 3z_1 - 3z_2 + z_3, \quad \widehat{b} = \frac{-5z_1 + 8z_2 - 3z_3}{2h}, \quad \widehat{c} = \frac{z_1 - 2z_2 + z_3}{2h^2}. \tag{35}$$

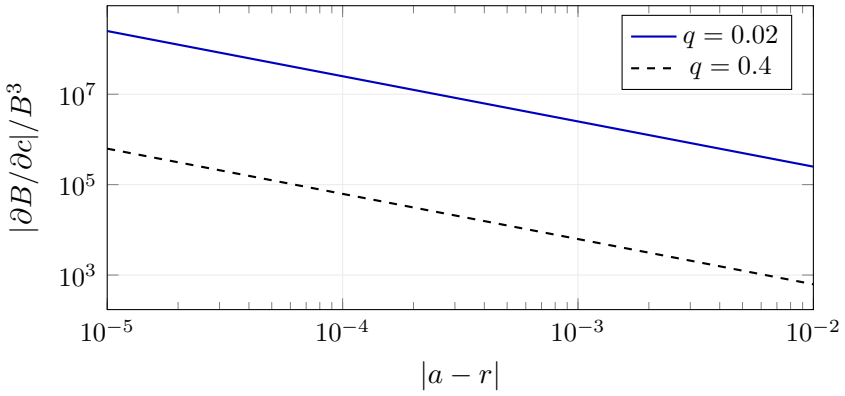



Figure 2: Local sensitivity of the reconstructed heavy scale to an absolute error in $cB^2$. Here $B$ in the normalization is fixed at its baseline value, and $r, b$ are held fixed in the derivative. The exact expression $1/[q^2|a - r|]$ diverges at the non-identifiable locus. The $q = 0.4$ curve illustrates the classical inverse problem; it is not a weak-background EFT example on $a = r$, where $|Cv^2| = q/2$.

Each normalized data error is bounded by $\epsilon_y/(ih) + K_4(ih)^3/24$. Applying the absolute row sums of these interpolation weights proves (30). At $a = r$ the true remainder vanishes, but structural non-identifiability of $B$ persists.

## C Exact algebraic and numerical verification

The accompanying scripts verify exact polynomial identities, finite-data matrix rank and local two-data fibres, calibrated residue inversion, interpolation weights, and deterministic error envelopes. Rational arithmetic is used for algebraic witnesses; a separate 70-digit decimal calculation checks the finite-fit bias. An independent adversarial check demonstrates the failure of a single uncalibrated residue and the amplification of small pointwise truncation errors by a fit. These checks support reproducibility; no numerical test replaces the proofs above.

## D A finite-data matrix error certificate

Fix a known reference mass $\mu$ and write $u_i = x_i/\mu^2$, $v_i = y_i/\mu^2$, $z_i = v_i/u_i$ and $p = (a, B/\mu^2, M/\mu^2)^T$. Equation (12) then uses the dimensionless rows $A_{i\cdot} = [u_i(1 - z_i), -z_i, 1]$ and $f_i = u_i z_i(1 - z_i)$. Suppose the squared momenta are known exactly and $|\widehat{v}_i - v_i| \le e_i$. Form $\widehat{A}, \widehat{f}$ and $\widehat{p} = \widehat{A}^{-1}\widehat{f}$ from the measured values. Set

$$E_A = \max_i e_i(1 + 1/u_i), \qquad E_f = \max_i \left[|1 - 2\widehat{z}_i|e_i + \frac{e_i^2}{u_i}\right]. \tag{36}$$

These bound $\|\widehat{A} - A\|_\infty$ and $\|\widehat{f} - f\|_\infty$. If $\alpha = \|\widehat{A}^{-1}\|_\infty E_A < 1$, the Neumann bound and the perturbed linear equation imply

$$\|p - \widehat{p}\|_\infty \le \frac{\|\widehat{A}^{-1}\|_\infty(E_f + E_A\|\widehat{p}\|_\infty)}{1 - \alpha} =: E_p. \tag{37}$$

This is a standard linear-system perturbation bound specialized to the spectral data. It assumes a true member of the model within the declared data-error intervals and does not establish model adequacy. Sufficient admissibility margins are $\widehat{a} > E_p$, $\widehat{M}/\mu^2 > E_p$ and

$(\widehat{B} - \widehat{M})/\mu^2 > 2E_p$. Failure of $\alpha < 1$ makes this bound inconclusive; it is not evidence of a physical instability or of nonexistence. If the error intervals contain an exactly exceptional model, its true matrix is singular and $\alpha < 1$ cannot hold: apparent rank induced by noise cannot evade the exceptional fibre. Momentum-calibration errors require a separate model.

## Data and code availability

The accompanying local reproduction package contains the verification code, exact test inputs, figure tables and build instructions. The figures use generated model values, not observational data. No external data repository or public release is asserted.

## References


[1] Giulia Gubitosi, Federico Piazza, and Filippo Vernizzi. The effective field theory of dark energy. *JCAP*, 02:032, 2013. doi: 10.1088/1475-7516/2013/02/032. URL https://arxiv.org/abs/1210.0201v2.

[2] David Langlois, Sébastien Renaux-Petel, Danièle A. Steer, and Takahiro Tanaka. Primordial perturbations and non-gaussianities in DBI and general multi-field inflation. *Phys. Rev. D*, 78:063523, 2008. doi: 10.1103/PhysRevD.78.063523. URL https://arxiv.org/abs/0806.0336v1.

[3] Frederico Arroja, Shuntaro Mizuno, and Kazuya Koyama. Non-gaussianity from the bispectrum in general multiple field inflation. *JCAP*, 08:015, 2008. doi: 10.1088/1475-7516/2008/08/015. URL https://arxiv.org/abs/0806.0619v1.

[4] Ana Achúcarro, Vicente Atal, Sebastián Céspedes, Jinn-Ouk Gong, Gonzalo A. Palma, and Subodh P. Patil. Heavy fields, reduced speeds of sound and decoupling during inflation. *Phys. Rev. D*, 86:121301, 2012. doi: 10.1103/PhysRevD.86.121301. URL https://arxiv.org/abs/1205.0710v2.

[5] Rhiannon Gwyn, Gonzalo A. Palma, Mairi Sakellariadou, and Spyros Sypsas. Effective field theory of weakly coupled inflationary models. *JCAP*, 04:004, 2013. doi: 10.1088/1475-7516/2013/04/004. URL https://arxiv.org/abs/1210.3020v2.

[6] Toshifumi Noumi, Masahide Yamaguchi, and Daisuke Yokoyama. Effective field theory approach to quasi-single field inflation and effects of heavy fields. *JHEP*, 06:051, 2013. doi: 10.1007/JHEP06(2013)051. URL https://arxiv.org/abs/1211.1624v3.

[7] Lucas Pinol, Sébastien Renaux-Petel, and Denis Werth. The cosmological flow: A systematic approach to primordial correlators, 2023. URL https://arxiv.org/abs/2312.06559v1.

[8] Rhiannon Gwyn, Gonzalo A. Palma, Mairi Sakellariadou, and Spyros Sypsas. On degenerate models of cosmic inflation. *JCAP*, 10:005, 2014. doi: 10.1088/1475-7516/2014/10/005. URL https://arxiv.org/abs/1406.1947v2.

[9] Joe Kennedy, Lucas Lombriser, and Andy Taylor. Reconstructing horndeski models from the effective field theory of dark energy. *Phys. Rev. D*, 96:084051, 2017. doi: 10.1103/PhysRevD.96.084051. URL https://arxiv.org/abs/1705.09290v2.

[10] J. C. Criado and M. Pérez-Victoria. Field redefinitions in effective theories at higher orders. *JHEP*, 03:038, 2019. doi: 10.1007/JHEP03(2019)038. URL https://arxiv.org/abs/1811.09413v2.